

CHAPTER 4

EXPERIMENTAL SETUP AND PROCEDURE

The experimental setup with necessary instruments to evaluate the performance, emission, and combustion characteristics of the diesel engine at different operating parameters is shown in Figure 4.1. In this chapter, the instruments which were used in the experiments and the experimental procedures followed in this study are detailed.

4.1 DESCRIPTION OF ENGINE

The Kirloskar make engines are one of the widely used engines in the agricultural sectors. Apart from agricultural sectors, they are also used in heavy duty industrial applications like mining industries, construction industries and in automotive sectors. The piston of these engines is designed to have centralised cavity and also the piston is continuously cooled by built-in oil jet spray for minimum wear of the liner of the piston (Kirloskar 2014). The rigid structure of the engine also ensures minimum cylinder bore distortion when the engine is operated at high in-cylinder pressures. Further, it is easier to make any necessary modifications in the cylinder head and piston crown of the engine.

The present experimental investigation was conducted in a Kirloskar make single cylinder, water-cooled, four stroke, DI diesel engine, developing a rated power of 5.9 kW at a speed of 1800 rpm and having a compression ratio of 17.5:1. The detailed engine specification is given in Appendix 1. The experiments were conducted at a constant speed of 1800 rpm with variable load. The load

ranged from no load condition to full load condition (0% to 100% rated load of the engine with the steps of 25%). The operating parameters such as injection time of diesel fuel and injection pressure of the diesel fuel recommended by the manufacturer are 23°BTDC and 200 bar injection pressure. The governor of the engine was used to control the engine speed. The engine was cooled by supplying the water through the jackets of the engine block and the cylinder head.

An arrangement was made in a cylinder head to fit a piezoelectric pressure transducer for measuring the in-cylinder pressure. For loading the engine, the engine was coupled with eddy current dynamometer. Figure 4.2 illustrates the schematic arrangement of the experimental set up.



Figure 4.1 Photographic view of experimental set up

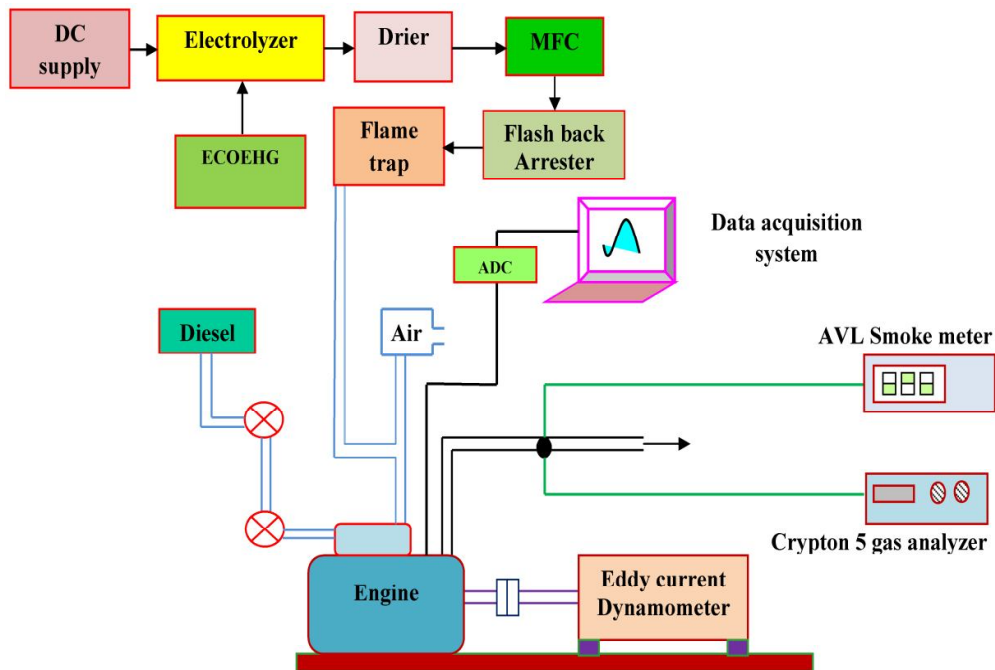


Figure 4.2 Schematic diagram of experimental set up

4.2 INSTRUMENTS USED

The different instruments used in this experimental investigation are detailed in this section.

4.2.1 Torque Measurement

The dynamometer was used in this experimental investigation to load the engine thereby the torque could be measured. It was of high speed type eddy-current dynamometer. Figure 4.3 depicts the control panel of eddy current dynamometer. The eddy current dynamometer works on the principle that an electrically conductive shaft or disc moving through a magnetic field will create a resistance to that movement. The dynamometer has a toothed rotor and is driven

by the engine. The magnetic poles are located outside of it with a gap. These magnetic poles are excited by the coil which is wound in circumference direction. When the current passes through this exciting coil, the magnetic flux ring is formed around this coil through stators and rotors. Owing to density difference created by the rotation of rotor, the eddy-current flows to stator. These eddy currents resist the rotor motion which results in the loading of the engine. The strain gauge is provided in the eddy current dynamometers for direct torque measurement. The technical specification of the eddy current dynamometer is tabulated in Appendix 2.



Figure 4.3 Photographic view of control panel of eddy current dynamometer

4.2.2 Fuel Consumption Measurement



Figure 4.4 Photographic view of Panel board with burette

Figure 4.4 shows the photographic view of diesel fuel measurement system. The diesel was supplied to the engine from the tank which was fitted at the back of the panel board. The diesel consumption was measured by using a burette which was fitted at the front side of the panel board. To measure the diesel consumption, a three way valve was also fitted at the bottom of the burette. The diesel consumption was calculated on the basis of time taken by the engine to consume 10 cc of diesel.

4.2.3 Temperature Measurement

Temperature of the inlet air, exhaust gas, cooling water inlet and outlet were measured using K-Type thermocouples. They are made of Chromel and

Alumel. They can be used to measure temperatures from -200°C to 1350°C . They work on the principle of Seebeck effect. The working principle of thermocouple is shown in Figure 4.5.

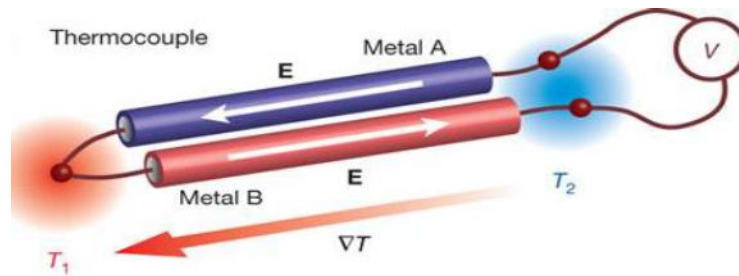


Figure 4.5 Principle of thermocouple – Seebeck effect (Seebeck 2014)

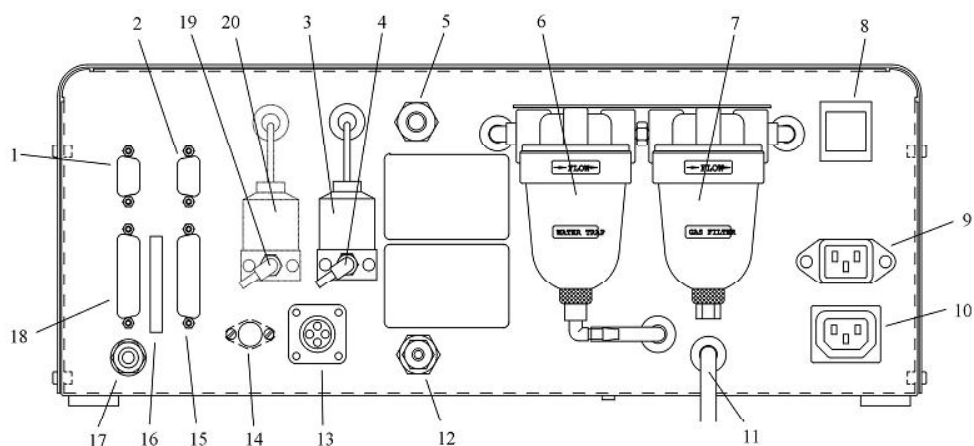
4.2.4 Exhaust Gas Measurement

Crypton 290 EN2 five gas analyzer was used to measure the exhaust gas emissions such as CO, CO₂, UBHC, NO_x, and excess oxygen. The photographic view of the analyzer is shown in the Figure 4.6.



Figure 4.6 Photographic view of exhaust gas analyzer

This is a fully microprocessor controlled exhaust gas analyser. This employs the principle of Non-Dispersive Infra-Red (NDIR) Technique for the measurement of gases like CO, CO₂, and UBHC. NO_x is measured by means of a chemical sensor which uses a catalyst for its measurement. The excess oxygen is measured on the principle of electro-chemical reaction which is widely used in fuelcells. This analyzer can be operated on a wide range of A.C. voltage of 100 to 250 volts and 50/60 Hz. The technical specification of the analyzer is given Appendix 3 and the external connections of the analyzer are shown in Figure 4.7.



1	RS232 Port - CMT Communications	11	Water Output
2	RS485/RS232 Communications (optional) Not Used	12	Sample Probe Input
3	Oxygen Sensor	13	Temperature Probe Input
4	Sample Exhaust	14	Keyboard Input
5	Calibration Gas Input	15	Parallel Port (optional) - Not Used
6	Water Trap and Primary Filter	16	Viewing Slot for status LEDs
7	Gas Filter	17	Tachometer Probe Input
8	Mains On/Off	18	Parallel port - printer
9	Mains Input	19	Sample Exhaust – NO _x (295 AND 297-5 ONLY)
10	Mains Auxiliary Output	20	NO _x Sensor (295 AND 297-5 ONLY)

Figure 4.7 External Connections of gas analyzer (Crypton 2005)

4.2.4.1 Measurement of Smoke

The smoke was measured by AVL smoke meter. The photographic view of the smoke meter is shown in Figure 4.8. This smoke meter works on the principle of light extinction method. It comprises of a flexible sampling hose with suitable exhaust gas probe. The sampling probe is interleaved in the exhaust manifold approximately 150 mm to 200 mm from the engine. The exhaust gas sample is allowed to pass through the tube which is about 46 cm in length. One end of the tube have a light source and the other end of the tube is fitted with a photo cell. The intensity of smoke is sensed by the quantity of the light passing through the smoke column. This smoke meter displays the smoke intensity in terms of Hatridge Smoke Unit (HSU). The technical specification of this smoke meter is given in Appendix 4.



Figure 4.8 Photographic view of smoke meter

4.2.5 Combustion Analysis

4.2.5.1 In-cylinder Pressure Measurement

The in-cylinder pressure was measured by using piezoelectric pressure sensor of air cooled type with an inline charge amplifier. The sensitivity of the sensor is 25 mV/bar. It can be used in the wide range of pressures from 0 to 100 bar. The other technical specifications of the sensor are given in Appendix 5. This sensor was connected to the inline charge amplifier with a strong integrated high temperature Viton cable. They work on the principle that when a quartz crystal is squeezed by applying force, a charge is developed across the crystal. This developed charge is proportional to the force applied. The basic concept of piezoelectric pressure sensor is shown in Figure 4.9.

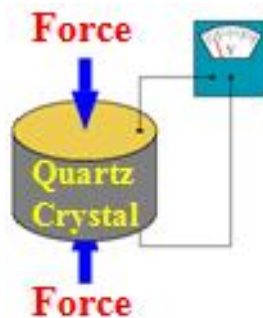


Figure 4.9 Basic concept of piezoelectric pressure sensor

4.2.5.2 Charge amplifier

A charge amplifier is a device which is always used along with pressure transducer to amplify the charge from one form to another. This amplifier

converts the input charge received from a sensor to a readable voltage output. The schematic circuit of piezoelectric transducer with inline charge amplifier is shown in Figure 4.10.

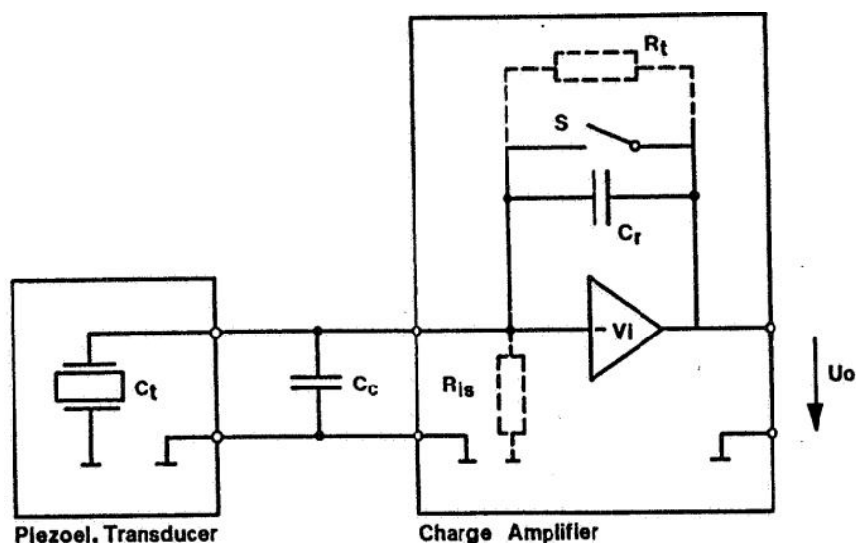


Figure 4.10 Circuit schematic of piezoelectric transducer with inline charge amplifier (Mahr & Gautschi 2012)

4.2.5.3 Crank Angle Measurement

For the measurement of in-cylinder pressure with respect to crank position a crank angle detector assembly was used. This consisted of a crank angle marker, an electromagnetic pickup and a signal processing unit. The Figure 4.11 depicts the photographic view of the crank angle detector assembly. This assembly was mounted on the crank shaft of the test engine. The output signal generated from crank angle detector assembly was sent to signal conditioner.



Figure 4.11 Photographic view of crank angle detector

4.2.5.4 Combustion Analyzer

The efficient and effective method to evaluate the combustion characteristics of the engine could be carried out by using an engine combustion analyzer. The photographic view of the combustion analyzer is shown in Figure 4.12.



Figure 4.12 Photographic view of combustion analyzer

It is a rugged and a compact one. By using this analyzer the combustion parameters such as indicated power, pressure-volume and pressure-crank angle diagrams, 5% mass fraction burnt angle, 95% mass fraction burnt angle, gross IMEP, maximum heat release rate, maximum heat release rate crank angle, maximum pressure, maximum pressure crank angle, etc., could be measured.

4.2.5.5 Data acquisition system

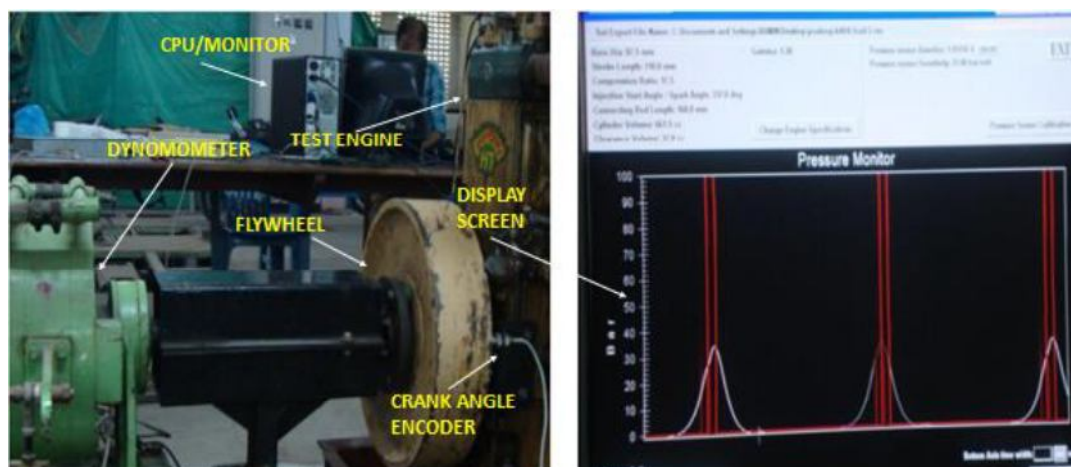


Figure 4.13 Photographic view of data acquisition system

Engine Test Express is a windows based controlling software. This software was used in the data acquisition system. By using this software the real time data measurement of the in-cylinder processes, auto zooming of graphs, analog and digital display of data in the computer, storing of data for future analysis could be made with ease. Also, by using this software the data could be exported directly to Microsoft excel. This data acquisition software was developed

by LEGION BROTHERS, India. The photographic view of the data acquisition system is shown in Figure 4.13.

4.3 OEH GAS INDUCTION



Figure 4.14 photographic view of OEH gas induction point

Figure 4.14 shows the photographic view of OEH gas induction point which was provisioned in the inlet manifold of the engine.

4.3.1 Generation of OEH gas

In this experimental investigation OEH gas was generated by electro-chemical dissociation of water. Figure 4.15 displays the basic concept of the process.

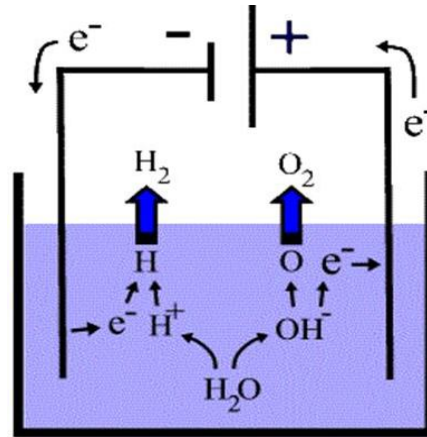


Figure 4.15 Basic electrolysis process (Power 2014)

4.3.1.1 DC Power Supply

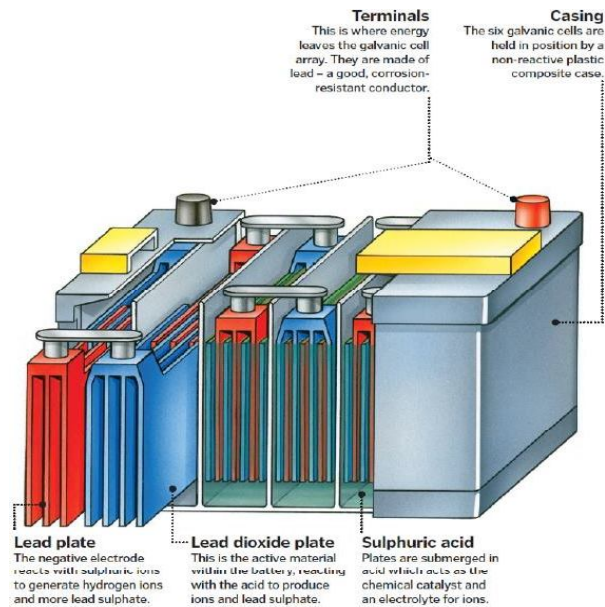


Figure 4.16 Cross sectional view of lead acid battery (Lead 2014)

DC power of 12V was supplied to the electrolysis unit. For this purpose separate lead acid battery of 12V was used. The cross sectional view of battery showing the innards of the battery is shown in the Figure 4.16.

4.3.1.2 Process of Electrolysis

For generating OEH gas by electrochemical reaction, the process needs an electrolyzer for the separation of water. This consists of the electrolysis chamber, an aqueous electrolytic solution comprising water and electrolyte. In this experimental investigation, sodium hydroxide (NaOH) was used as electrolyte. This was due to its better characteristics than other electrolytes. The aqueous electrolyte solution of NaOH was filled in an electrolysis chamber such that $\frac{3}{4}$ of the electrolysis chamber was filled with aqueous electrolyte solution and $\frac{1}{4}$ of the electrolysis chamber above the aqueous electrolyte solution was left empty to use this space as a gas collection chamber. The electrodes stack consisted of two types of electrodes comprising anode electrodes and cathode electrodes. These electrodes were made of stainless steel 316L material since; stainless steel 316L material was much more corrosion resistant than other electrode materials. In the electrolyzer, the anode electrode and the cathode electrode were placed sequentially with a gap of 2 mm between them. OEH gas production primarily depended on the following factors:

- Gap between the electrodes
- Surface area of the anode and cathode electrodes
- Concentration of aqueous electrolyte solution
- Potential difference applied between the anode and cathode electrodes

The electrodes stack was immersed in the aqueous electrolyte solution with their positive and negative leads out. When electrical potential was applied across the electrodes of the electrolyser, water was directly transmuted into oxygen enriched hydrogen gas. This was collected in the gas collection chamber and delivered through the flexible hose to the intake manifold of the diesel engine. Before letting to the intake manifold, the OEH gas was passed through the drier, flash back arrestor, and flame trap to avoid any accident/damage in case of back firing of the engine. Table 4.1 shows the constituents of OEH gas and the properties of OEH gas is given in Table 4.2.

Table 4.1 Constituents of OEH gas

Constituent of OEH gas	Percentage
Hydrogen (H ₂)	64.03
Oxygen (O ₂)	31.87
Others (H, O, OH, H ₂ O)	4.1

Table 4.2 Properties of OEH gas

Property of OEH gas	Unit	Value
Density	kg/m ³	0.096
Specific gravity		0.078
Specific volume	m ³ /kg	12.76
Auto ignition temperature	K	743.6
Lower heating value	MJ/kg	94.42

4.3.1.3 Electrolysis unit

The photographic view of one of the electrolysis unit is shown in Figure 4.17.



Figure 4.17 Photographic view of one of the electrolysis unit

4.3.1.3.1 Electrolysis chamber

The electrolysis chamber is a space in the electrolyzer where the aqueous electrolyte solution of NaOH is filled. The electrolyte solution is filled in the electrolysis chamber such that $\frac{3}{4}$ of its space is filled with aqueous electrolyte solution and $\frac{1}{4}$ of the space in the electrolysis chamber above the aqueous electrolyte solution is kept empty to use this space as a gas collection chamber. The stack with anode electrodes and the cathode electrodes is placed in the

electrolysis chamber such that the stack is totally submerged in the electrolyte solution.

4.3.1.3.2 Electrodes

The electrodes stack in the electrolysis chamber consists of two types of electrodes. One is positively charged anode electrodes and the other one is negatively charged cathode electrodes. The photographic view of the stack of electrodes is shown in Figure 4.18.



Figure 4.18 Photographic view of stack of electrodes

These electrodes were made of stainless steel 316L material. In the initial stages of the experiments instead of stainless steel 316L electrodes, stainless steel 304 material was used for electrode. On continuous usage, grade 304 electrodes got corroded. The photographic view of the electrode is shown in Figure 4.19.



Figure 4.19 Photographic view of electrode

In the figure it is shown that the smooth surface of the electrode is made rough in order to increase the generation rate of OEH gas. It is experimentally found that the gas generation capacity of the electrodes with smooth surface is always less than the generation capacity of the electrodes with rough surface. This is because when the surface is smooth, the active surface areas get reduced and this eventually lessens the generation capacity of the cell. In the initial stages of this experimental investigation, various electrode designs were analysed for their efficiency of generation of OEH gas. The electrode having the combination of circular plate and the square plate gave higher efficiency compared to other shapes of electrodes. The photographic view of the various shapes of electrodes is shown in Figure 4.20.



Figure 4.20 Photographic view of various shapes of electrode

4.3.1.3.3 Aqueous Electrolytic Solution

The aqueous electrolytic solution consists of water and electrolyte. Pure water is actually an insulator. It will not conduct electricity. To make the water a better conductor, electrolyte is needed. Some of the electrolytes which can be used in the electrolysis process are potassium hydroxide (KOH), potassium hydrate (H_2KO), sodium hydroxide (NaOH), sodium bicarbonate (NaHCO_3), sodium chloride (NaCl) & vinegar. In this study NaOH was used as electrolyte. This was due to its better characteristics than other electrolytes.

4.3.1.4 Electronic control unit of OEH gas

The assembled view of the electronic control unit of OEH gas (ECOEHG) is shown in the Figure 4.21. It works on the principle of Pulse Width Modulator (PWM). The main feature of PWM is that it can control the intensity of power sent to a load. Owing to this feature, the generation rate of OEH gas can be

varied according to the requirement. This increases the production efficiency of the electrolyzer. Figure 4.22 depicts the basic concept of PWM.



Figure 4.21 Electronic control unit of OEH gas

In Figure 4.22, the top portion shows a PWM output of 20% duty cycle. It means that the signal is on for 20% of the period and off for the remaining 80% of the period. The middle portion shows a PWM output of 50% duty cycle. It means that the signal is on for 50% of the period and off for the remaining 50% of the period. The lower portion shows a PWM output of 80% duty cycle.

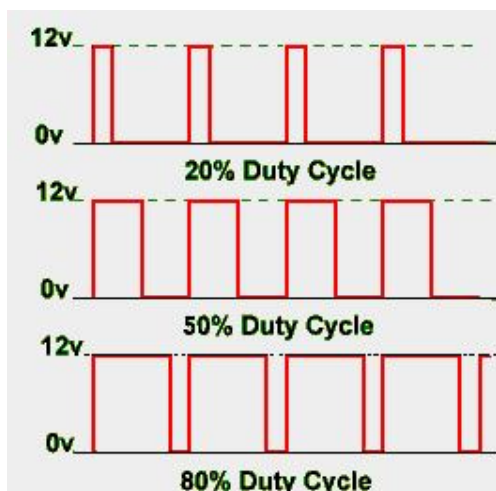


Figure 4.22 Basic concept of PWM (PWM 2014)

It means that the signal is on for 80% of the period and off for the remaining 20% of the period. From the figure, it can be concluded that the power input to the load can be effectively varied according to the requirement by using PWM. In the present work Constant Current PWM is used which can be abbreviated CCPWM. The main difference being compared to other normal modulator is that in this type, the amount of current which can be used to produce OEH gas can be fixed. Due to this feature, the quantity of current can be varied according to the amount of OEH gas required. One more advantage of using this type of modulator is that according to the preset value of the current, the system itself will control the duty cycle. Owing to this the OEH gas generation can be precisely controlled and also the electrolysis unit can be prevented from Current Runaway. When the electrolysis unit runs, it warms up over time, and as it warms up, it draws more amperage and this is called current runaway. If it is not prevented it will damage the entire system.

Table 4.3 shows the power requirement to produce various flow rates of OEH gas.

Table 4.3 Power requirement of OEH gas production

OEH flow rate (lpm)	Power required (W)
1.2	72
2.4	120
3.7	180
4.6	240
5.5	276

4.3.1.5 Safety devices

Before inducting to the intake manifold of the engine, the OEH gas was passed through a flashback arrestor and a flame trap to avoid any accident/damage in case of back firing of the engine. The flashback arrestor used in this experiment was of wet type and the flame trap was of dry type. The photographic view of a flashback arrestor is shown in Figure 4.23.

A flashback arrestor is a cylindrical container containing water with a provision for connecting two hoses. One connects with the electrolyzer; it allows the OEH gas to bubble up through the water in the tube, and another one is connected to the inlet manifold of the engine after passing through the flame trap.

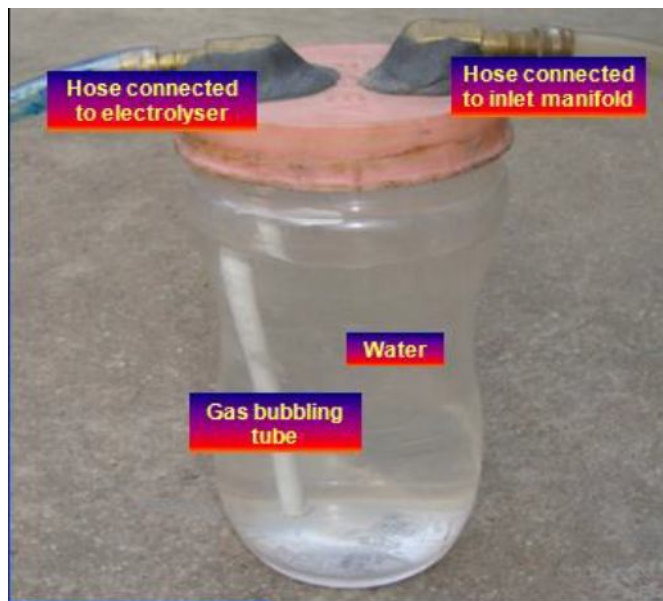


Figure 4.23 Photographic view of flashback arrestor



Figure 4.24 Photographic view of flame trap

The photographic view of a flame trap is shown in Figure 4.24. Flame trap is made of brass pipe. It is densely filled with bronze wool to eliminate flame propagation while still allowing the unrestricted flow of OEH gas. This highly dense bronze wool reduces the gas pressure, slows down the flame front, and cooling the gases below ignition temperature thereby it inhibits flame propagation, when back fire from the engine occurs. In initial stages instead of brass wool steel

wool was used in the experimental investigation. Figure 4.25 shows the condition of steel wool before and after the occurrence of back fire from the engine.



Figure 4.25 Photographic view of steel wool before and after backfire from engine

4.3.1.6 OEH Gas Measurement

The OEH gas was metered out through a digital mass flow controller (MFC) of Aalborg make. The principle of operation of MFC is that the temperature differential existing between two streams of the same gas is proportional to the change in resistance of the sensor windings which in turn calculates the flow rate of the gas. The principle of operation of MFC is shown in Figure 4.26.

In MFC the metered gases are divided into two streams of laminar flow. One is sending through the prime flow passage. Another one is through a capillary tube sensor. Both flow passages are designed for laminar flows and hence their ratio of flow rates is also constant. When the sensing winding on the sensor tube is heated, the gas passing through the tube gets heated. The resultant temperature differential between the gas passing through prime flow and that

passing through sensor tube is proportional to the flow rate of gas. The technical specification of the MFC is given in Appendix 6.

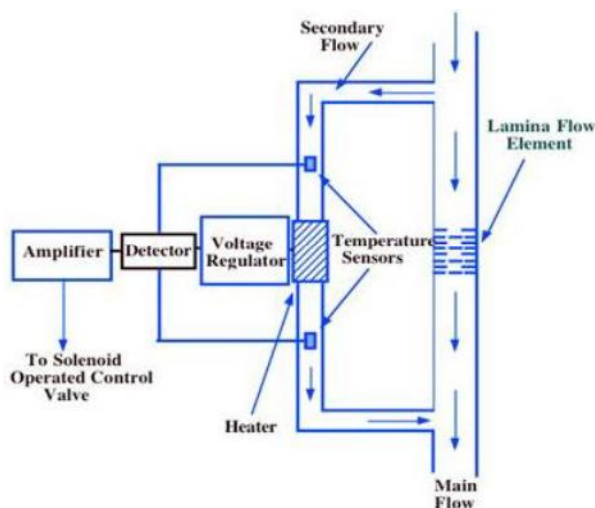


Figure 4.26 Principle of operation of MFC (MFC 2014)

4.4 EXPERIMENTAL PROCEDURE

Prior to the conduct of the engine experiments, the fuel tank, engine oil level, coolant, dynamometer, all analyzers and meters were checked. The test engine was cranked and warmed up for an hour. Simultaneously, the dynamometer, all analyzers and meters for measurements attached to the engine were switched on and the proper preparations and settings for measurements were made as recommended by the manufacturers of the instruments. After attaining the stable condition, the load on the engine was increased gradually from 0% to 100% in steps of 25%. The engine speed at all load conditions was adjusted for constant engine speed of 1800 rpm. In each load condition, the measurements of fuel consumption, intake air temperature, exhaust gas temperature, engine cooling water temperature at inlet and outlet, in-cylinder pressure, crank angle, and

engine-out emissions like carbon monoxide (CO), carbon dioxide (CO₂), unburned hydrocarbon (UBHC), oxides of nitrogen (NO_x), excess oxygen (O₂) and smoke were recorded. All the measurements were repeated thrice and the average value was taken for analysis.

Initially the engine was tested with petroleum diesel at standard engine specifications i.e., injection timing of diesel fuel as 23° BTDC, injection pressure as 200 bar, compression ratio as 17.5:1, and speed as 1800 rpm. This served as a base line operation to compare the results of other experiments.

In the first of phase of experiment, the engine was tested for the best flow rate of OEH gas by considering the facts of higher thermal efficiency and reduced engine-out emissions. For this, the OEH gas of 1.2 litre per minute (lpm), 2.4 lpm, 3.7 lpm, 4.6 lpm, and 5.5 lpm produced by electrochemical reaction of water were aspirated into the cylinder along with the intake air at standard engine specification.

Then for the best flow rate of OEH gas, six operating parameters of the engine were varied and tested for their impact on performance, emission, and combustion characteristics of the engine. The six operating parameters varied were:

- Injection time of diesel fuel
- Injection pressure of diesel fuel
- Temperature of diesel fuel
- Inlet air temperature
- Cooling water flow rate
- Combination of injection pressure and injection time of diesel fuel

After the completion of the engine experiments, the experimental data were processed and analyzed.

4.5 EXPERIMENTAL UNCERTAINTY

In the present experimental investigation, many physical quantities were measured using various instruments. All the instruments were calibrated prior to their use. Uncertainties for the present experimental work are detailed in Table 4.4.

Table 4.4 Experimental uncertainties

Variable	Uncertainty
Speed	± 1 rpm
Temperature	$\pm 1^\circ$
Time	± 0.1 s
Pressure	± 0.6164 %
Brake power	± 0.9434 %
Fuel flow	± 0.7319 %
NO _x	± 10 ppm
CO	± 0.01 %
CO ₂	± 0.03 %
UBHC	± 1 ppm
Smoke	± 1 HSU

The uncertainties for basic measurements like temperature, speed, time etc., were taken as the value of least count of relevant instruments. The errors on

quantities such as CO, CO₂, UBHC, NO_x, O₂, smoke were taken from manuals supplied by the manufactures of instruments. The uncertainty for derived quantities was computed on the basis of Holman's (2000) method. This was based on the work of Kline & McClintock (1953).